# Convective Cahn-Hilliard Models: From Coarsening to Roughening

A. A. Golovin,[1] A. A. Nepomnyashchy,[2] S. H. Davis,[1] and M. A. Zaks[3]

[1]*Department of Engineering Sciences and Applied Mathematics, Northwestern University, Evanston, Illinois 60208-3100*

[2]*Department of Mathematics and Minerva Center for Nonlinear Physics of Complex Systems, Technion–Israel Institute of Technology, Haifa 32000, Israel*

[3]*Department of Nonlinear Dynamics, Institute of Physics, Potsdam University, D-14415, Potsdam, Germany*

(Received 6 September 2000)

In this paper we demonstrate that *convective* Cahn-Hilliard models, describing phase separation of driven systems (e.g., faceting of growing thermodynamically unstable crystal surfaces), exhibit, with the increase of the driving force, a transition from the usual coarsening regime to a chaotic behavior without coarsening via a pattern-forming state characterized by the formation of various stationary and traveling periodic structures as well as structures with localized oscillations. Relation of this phenomenon to a kinetic roughening of thermodynamically unstable surfaces is discussed.

DOI: 10.1103/PhysRevLett.86.1550 PACS numbers: 64.60.–i, 68.35.Ct, 68.35.Rh, 81.10.Aj

Convective Cahn-Hilliard models have recently been proposed to describe several physical processes: spinodal decomposition of phase separating systems in an external field [1–3], spatiotemporal evolution of the morphology of steps on crystal surfaces [4], and growth of thermodynamically unstable crystal surfaces with strongly anisotropic surface tension [5–8]. In the simplest one-dimensional case the model is described by the following equation:

$$u_t - Duu_x + (u - u^3 + u_{xx})_{xx} = 0, \qquad (1)$$

where subscripts denote partial derivatives, $u$ is the order parameter, and $D$ is the driving force; for instance, in the case of a growing crystal surface with strongly anisotropic surface tension, $u$ is the surface slope and $D$ is the growth driving force proportional to the difference between the bulk chemical potentials of the solid and fluid phases [5,7,8].

For small driving force $D \to 0$, Eq. (1) is reduced to the well-known Cahn-Hilliard (CH) equation describing spinodal decomposition in phase-separating systems [9] and exhibiting the coarsening dynamics [10] of which faceting of thermodynamically unstable surfaces is a well-known example [11,12]. With the growth of the driving force there must be a transition from the coarsening dynamics to a chaotic spatiotemporal behavior, since for $D \to \infty$ the transformation $u \to u/D$ reduces Eq. (1) to the well-known Kuramoto-Sivashinsky (KS) equation. Below we study in more detail the transition from the coarsening to the chaotic behavior in this convective Cahn-Hilliard model.

Equation (1) has exact solutions [1]

$$u_\pm(x) = u_\pm^0 \tanh u_\pm^0 x, \qquad u_\pm^0 = \sqrt{1 \pm D/\sqrt{2}}, \qquad (2)$$

for $D > -\sqrt{2}$ and $D < \sqrt{2}$, corresponding to a valley (positive kink) and a hill (negative kink), respectively. In the following we shall assume $D > 0$ (otherwise, the transformation $x \to -x$ is performed). One can see that a valley is sharper than a hill and the surface growth destroys usual double-tangent construction [7,8].

On a periodic domain, the final result of the coarsening would be a single kink-antikink (hill-valley) pair. However, for $D > \sqrt{2} = 1.41$ such a solution does not exist. Moreover, the far-field hill solution (2), $(u_-^0)^2 = 1 - D/\sqrt{2} = \text{const}$, becomes unstable for $D > 2\sqrt{2}/3 = 0.94$. Thus for $D > 0.94$ a single kink-antikink pair cannot persist.

Consider now bounded stationary solutions $u = u(x)$ of Eq. (1) in the infinite region $-\infty < x < \infty$ that satisfy the ordinary differential equation

$$u_{xxx} + (u - u^3)_x - \frac{1}{2} Du^2 = -\frac{1}{2} DA, \qquad (3)$$

where $A = \langle u^2 \rangle \equiv \lim_{L\to\infty} \int_{-L}^{L} u^2\, dx$ is a constant. When $A = A_* = 1 - D/\sqrt{2}$, there exists a heteroclinic loop connecting the fixed points $P_\pm$ which correspond to constant solutions $u = \pm\sqrt{A_*}$. Indeed, the linearization of (3) near the fixed points $P_\pm$ gives the following equation for the eigenvalues: $\lambda^3 + \lambda(1 - 3A_*) \mp D\sqrt{A_*} = 0$. One can see that for $D < D_0 = \sqrt{2}/3 = 0.47$ the eigenvalues are real. The dimension of the unstable manifold of the point $P_+$ ($P_-$) is the same as that of the stable manifold of $P_-$ ($P_+$), and equal to 1 (2). The trajectory formed by the intersection of the stable manifold of $P_+$ and the unstable manifold of $P_-$, together with the negative kink (2), form a heteroclinic loop. When $A < A_*$, the heteroclinic loop is destroyed, and a long-period limit cycle appears. Numerical calculations show [13] that for $0 \le D < D_0$ there exists a family of stationary spatially periodic solutions with $0 < \langle u^2 \rangle < A_*$, for which $\langle u^2 \rangle \equiv A$ is a monotonically decreasing function of the wave number $k = 2\pi/l$, $dA/dk < 0$, where $l$ is the spatial period; as $k \to 0$, $A \to A_* = 1 - D/\sqrt{2}$; as $k \to 1$, $A \to 0$.

The stability of stationary periodic solutions $u(x)$ is determined by the eigenvalues $\sigma(\tilde{k}, D)$ of the problem

 0031-9007/01/86(8)/1550(4)$15.00 

$$\sigma\tilde{u} - D(u\tilde{u})_x + [\tilde{u}_{xx} + (1 - 3u^2)\tilde{u}]_{xx} = 0, \quad (4)$$

for a perturbation $\tilde{u}(x) = v(x;\tilde{k})e^{i\tilde{k}x}, v(x + l;\tilde{k}) = v(x;\tilde{k})$ in the form of Floquet functions bounded in the infinite region. The translational mode corresponds to $\sigma(0, D) = 0, v(x;0) = u_x$. In the limit of small $\tilde{k}$, the expansion $\sigma(\tilde{k}) = \sigma_1\tilde{k} + \sigma_2\tilde{k}^2 + \ldots$ can be used. An analysis similar to that performed in the case of KS equation [14] shows that, for $dA(k)/dk < 0$, $\sigma_1^2$ is positive, therefore all stationary periodic solutions in the infinite region are unstable (as in the case of CH equation).

We have performed a numerical simulation of Eq. (1) with periodic boundary conditions in a large domain, $L = 80\lambda_c$, where $\lambda_c = 2\pi\sqrt{2}$ is the preferred wavelength given by the linear theory, and found that for $D < D_0$ the kink coarsening takes place. It was observed that after the formation of initial periodic structure with the characteristic wave number $k_c = \sqrt{2}/2$, the structure undergoes the power-law coarsening $\langle L\rangle \propto t^{0.45}$, where $\langle L\rangle$ is the mean kink width averaged over the domain and ten random initial data (see Fig. 1). The coarsening rate slightly differs from that obtained in [3] for a dynamical system describing interacting kinks ($\sim t^{0.5}$). At the very late stages, crossover to a very slow coarsening has been observed. This late-stage coarsening is probably logarithmically slow, since our preliminary computations show that interaction of kinks at large distances is exponentially weak.

For $D > D_0$, the points $P_\pm$ become saddle-focus points, and our computations show that the dependence $A(k)$ for stationary solutions is not monotonic, which permits the stability of stationary solutions in a certain interval of wave numbers. We have found two types of stationary periodic solutions. One type is shown in Fig. 2a. The wavelength of this pattern decreases with the increase of $D$ as shown in Fig. 2b. In the case of a growing crystal surface, this corresponds to the formation of periodic hill-and-valley surface relief $h = \int u\,dx$.

Another type of stationary periodic solution is shown in Fig. 3a and 3b. One can see that this consists of two "elements": an "up" and a "down," one obtained from the other by inversion. The sequence of "ups" and "downs" can be arbitrary, as shown in Figs. 3a and 3b, but for stationary solutions of this type the numbers of "up" and "down" elements are always equal. The described two types of solutions can also form a composite stationary structure shown in Fig. 3c.

Besides stationary solutions, we have observed various nonstationary solutions, the simplest type being traveling waves. A typical traveling wave is shown in Fig. 3d. It also consists of "up" and "down" elements. However, the numbers of "ups" and "downs" in traveling waves are always different. Moreover, "up" and "down" elements are slightly asymmetric in this case, which leads to the appearance of large regions of nonzero mean slope of the surface shape $h$ (see below).

A more interesting nonstationary solution occurs when a sequence of "ups" and "downs" has defects. In this case one observes a structure which, on the whole, is either stationary or traveling, with the defects undergoing fast localized oscillations. Examples of such solutions are shown in Fig. 4.

The described stationary and traveling wave structures were observed for $D_0 \le D \le D_1$, where $D_1 \approx 7$. For smaller $D$ within this interval structures of the type shown in Fig. 2a prevail, while with the increase of $D$ the structures composited of "up" and "down" elements shown in Fig. 3 become typical. It is interesting that for larger $D$, starting from random initial data, one first observes irregular spatiotemporal behavior which, after some time, undergoes a transition to one of the described periodic solutions: a stationary solution, a traveling wave, or one of those with localized oscillating defects. The larger the $D$, the longer the initial period of the irregular behavior. In this regime, the solution consists of cells which evolve on two time scales: on the fast time scale they oscillate around their "quasiequilibrium" positions, while on the slow time scale they split and merge together, which is typical of KS dynamics. For $D > D_1$ we have not observed any transition to a regular behavior, and the observed irregular spatiotemporal dynamics is qualitatively similar to that of the KS equation, when cell oscillations, splitting and merging, all occur on the same time scale.

A transition from the coarsening dynamics to the chaotic behavior without coarsening is also observed in 2D

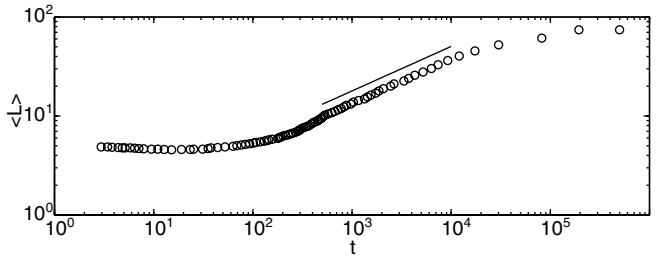


FIG. 1. Increase of the mean size of kink-antikink structure in time for the solution of Eq. (1) for $D = 0.2$, averaged over ten random initial data. The line corresponds to $t^{0.45}$.

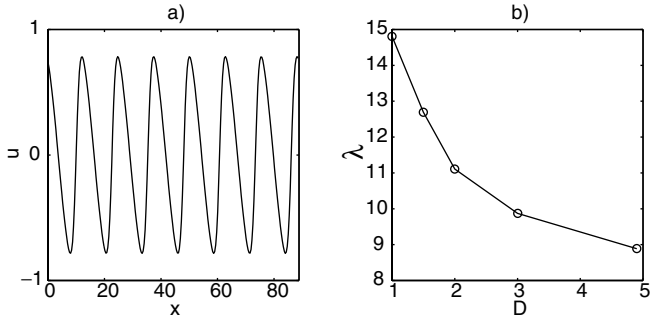


FIG. 2. (a) Stationary solution of Eq. (1) for $D = 1.5$; (b) dependence of the solution wavelength on $D$.

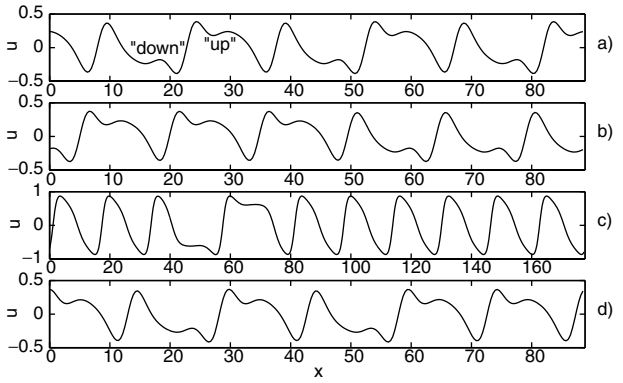


FIG. 3. Solutions of Eq. (1): stationary, consisting of "up"s and "down"s, (a) $D = 4.8$, (b) $D = 5.0$; (c) stationary "composited," $D = 1.0$; (d) traveling wave, $D = 4.7$ (travels to the left).

convective Cahn-Hilliard models. An interesting realistic example is the growth of a two-dimensional thermodynamically unstable crystal surface with strongly anisotropic surface tension. In the simplest case of thermodynamically unstable [001] surface, the evolution of the surface shape $h(x, y, t)$ can be described, after some rescaling, by the following equation [8]:

$$h_t = \frac{1}{2} D\,|\nabla h|^2 - \nabla^2 h - \nabla^4 h + 3(h_x^2 + \alpha h_y^2) h_{xx} + 3(\alpha h_x^2 + h_y^2) h_{yy} + \beta h_x h_y h_{xy}\,, \tag{5}$$

where $D$ is the growth driving force, and $\alpha$ and $\beta$ are the anisotropy coefficients of the crystal surface tension. In the 1D case, $h = h(x, t)$, Eq. (5) is transformed into Eq. (1) by writing $u = h_x$.

Equation (5) preserves the [001] symmetry, $x \to -x$, $y \to -y$, $x \to y$, and for small $D$ has solutions in the form

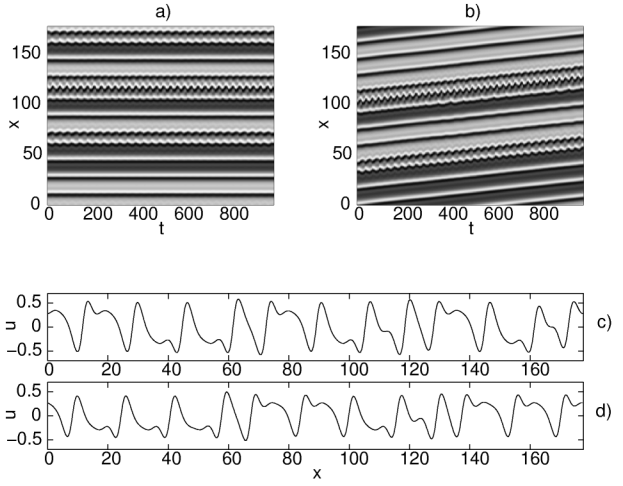


FIG. 4. Stationary (SO) and traveling (TO) solutions of Eq. (1) with localized oscillations. Spatiotemporal diagrams: (a) SO ($D = 3.0$), (b) TO ($D = 3.9$). Snapshots: (c) SO ($D = 3.0$), (d) TO ($D = 3.9$).

of square pyramids which undergo fast coarsening dynamics $\sim t^{0.47}$ [8], which is very close to that observed in the 1D case. Far from the corners, for $y \to -\infty$, the pyramid shape is described by

$$h \sim By - \sqrt{2}\ln[\cosh(Bx/\sqrt{2})] + vt\,, \tag{6}$$

where $B = \sqrt{(1 - D/\sqrt{2})/(1 + 3\alpha)}$, $v = D(1 - D/\sqrt{2})/(1 + 3\alpha)$. If $\alpha = 0$, Eq. (5) has an exact solution [8] in the form of a single square pyramid,

$$h = -\sqrt{2}\ln[\cosh(Bx/\sqrt{2})\cosh(By/\sqrt{2})] + vt\,. \tag{7}$$

As in the 1D case, for $D > \sqrt{2}$ the pyramid solution does not exist. However, before the growth driving force reaches this value, the pyramid becomes unstable. Linear stability analysis of the side of the pyramid, $h \sim B(x + y)$, gives the following dispersion relation for the harmonic perturbation growth rate $\sigma$ as a function of the wave vector $\mathbf{k} = (k_x, k_y)$:

$$\sigma = iDB(k_x + k_y) + \mathcal{Q}(k_x, k_y) - k^4, \tag{8}$$

where the quadratic form

$$\mathcal{Q}(k_x, k_y) = [1 - 3B^2(1 + \alpha)](k_x^2 + k_y^2) - \beta B^2 k_x k_y\,. \tag{9}$$

According to (8), the far-field pyramidal side is stable for

$$D < \frac{2\sqrt{2}}{3}\left[\frac{1 - |\beta|/4}{1 + \alpha - |\beta|/6}\right], \qquad |\beta| < 6(1 + \alpha)\,, \tag{10}$$

when the quadratic form $\mathcal{Q}$ is negative definite, and is unstable for all orientations of the wave numbers for

$$D > \frac{2\sqrt{2}}{3}\left[\frac{1 + |\beta|/4}{1 + \alpha + |\beta|/6}\right], \tag{11}$$

when the quadratic form $\mathcal{Q}$ is positive definite. For $|\beta| > 6(1 + \alpha)$ the pyramids are unstable for all $D$. This instability leads to the reorientation of the pyramidal structures, independently of the growth driving force.

Figure 5 shows different types of the system behavior, depending on the growth driving force $D$, for the case $\alpha = \beta = 0$. Figures 5a and 5b correspond to $D = 0.2$, for which a single pyramid, described by Eq. (7), is stable. In this case, the system exhibits the formation of square pyramids which coarsen in time. Figures 5c and 5d correspond to $D = 1.0$, for which a single pyramid described by Eq. (7) is unstable. One observes the formation of squarelike hillocks which are moving slowly along the surface. The mean size of the hillocks does not change in time so that there is no coarsening in this case. Figures 5e and 5f exhibit a chaotic regime corresponding to

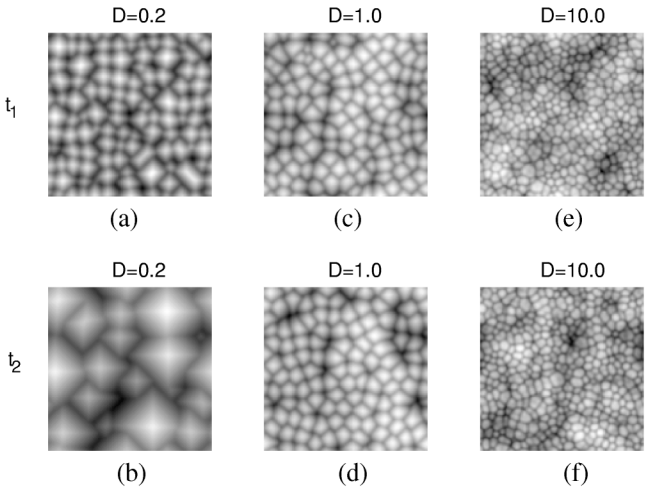


FIG. 5. Three types of surface dynamics observed with the increase of the growth driving force [solution of Eq. (5) for $\alpha = \beta = 0$]: coarsening of square pyramids, $D = 0.2$; square-shaped hillocks without coarsening, $D = 1.0$; chaotic surface, $D = 10.0$. The snapshots are shown for two different moments of time.

$D = 10$: hillocks do not have a square shape any more, and they merge and split in a chaotic manner typical of 2D Kuramoto-Sivashinsky dynamics. The crystal surface exhibits spatiotemporally chaotic relief.

An important and interesting question is whether the chaotic behavior of convective Cahn-Hilliard models for large driving force exhibits kinetic roughening. Since the KS equation, to which Eq. (1) is reduced for $D \to \infty$, exhibits in 1D large-scale roughening behavior of the KPZ (Kardar-Parisi-Zhang) universality class (see [15] and references therein), it is most likely that the observed transition from the coarsening dynamics to the KS-type chaotic behavior would provide a continuous model of the kinetic roughening transition for growing thermodynamically unstable faceted surfaces. Such a transition was observed in 1D Monte Carlo simulations [16]. Moreover, even for moderate driving forces when model (1) exhibits traveling waves consisting of "up" and "down" elements shown in Figs. 3 and 4, random sequences of slightly asymmetric "up"s and "down"s would yield, on large scales, a rough surface profile $h$. Figure 6 presents numerical solutions of Eq. (1) in large domain, $L = 80\lambda_c$, for $D = 3.0$ and $D = 10.0$, together with the corresponding surface profiles. The tendency to roughening can be easily seen both for $D = 3$ and $D = 10$.

It is less clear whether one would observe the roughening transition for the 2D convective Cahn-Hilliard model since large-scale roughening behavior of the 2D KS equation is still under discussion [15,17]. In the case of a growing thermodynamically unstable 2D crystal surface, an important factor is the *anisotropy* of the surface dynamics [17], as well as thermal noise. We shall study the roughening properties of such convective Cahn-Hilliard models for large driving force in further investigations.

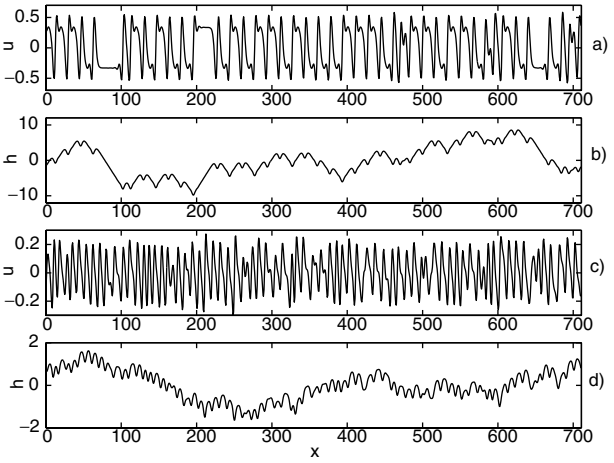


FIG. 6. Solutions of Eq. (1) for (a) $D = 3$ and (c) $D = 10$, and corresponding "rough" surface shapes, (b) and (d), respectively

This work was supported by Grant No. 9800086 from the Binational U.S.-Israel Science Foundation, by Technion V. P. R. Fund–P. and E. Nathan Research Fund, by the Fund for the Promotion of Research at the Technion, and by VW-Stiftung.

[1] K. Leung, J. Stat. Phys. **61**, 345 (1990).
[2] C. Yeung, T. Rogers, A. Hernandes-Machado, and D. Jasnow, J. Stat. Phys. **66**, 1071 (1992).
[3] C. L. Emmott and A. J. Bray, Phys. Rev. E **54**, 4568 (1996).
[4] Y. Saito and M. Uwaha, J. Phys. Soc. Jpn. **65**, 3576 (1996).
[5] F. Liu and H. Metiu, Phys. Rev. B **48**, 5808 (1993).
[6] M. E. Gurtin, *Thermomechanics of Evolving Phase Boundaries in the Plane* (Clarendon Press, Oxford, 1993).
[7] A. A. Golovin, S. H. Davis, and A. A. Nepomnyashchy, Physica (Amsterdam) **122D**, 202 (1998).
[8] A. A. Golovin, S. H. Davis, and A. A. Nepomnyashchy, Phys. Rev. E **59**, 803 (1999).
[9] J. W. Cahn and J. E. Hilliard, J. Chem. Phys. **28**, 258 (1958).
[10] K. Kawasaki and T. Ohta, Physica (Amsterdam) **116A**, 573 (1982).
[11] J. Stewart and N. Goldenfeld, Phys. Rev. A **46**, 6505 (1992).
[12] N. Cabrera, in *Proceedings of the Symposium on Properties of Surfaces* (American Society for Testing and Materials, Philadelphia, 1963), pp. 24–31.
[13] A. A. Golovin, S. H. Davis, A. A. Nepomnyashchy, and M. A. Zaks, in *Proceedings of Equadiff'99 Conference, Berlin, 1999* (World Scientific, Singapore, 2000).
[14] A. A. Nepomnyashchy, Fluid. Dyn. **9**, 586 (1974).
[15] T. Bohr, M. H. Jensen, G. Paladin, and A. Vulpiani, *Dynamical Systems Approach to Turbulence* (Cambridge University Press, Cambridge, England, 1998).
[16] D. G. Vlachos, L. D. Schmidt, and R. Aris, Phys. Rev. B **47**, 4896 (1993).
[17] B. M. Boghosian, C. C. Chow, and T. Hwa, Phys. Rev. Lett. **83**, 5262 (1999).